Heliyon 10 (2024) e33910

Contents lists available at ScienceDirect

Heliyon

journal homepage: www.cell.com/heliyon

Research article

A simulation study of irradiation effect on InAs/GaAsSb type II quantum dot structures

Guiqiang Yang [a,b], Yidi Bao [a,b], Xiaoling Chen [a,b], Chunxue Ji [a,b], Bo Wei [a,b], Wen Liu [a,b,c,**], Xiaodong Wang [a,b,c,*]

[a] Engineering Research Center for Semiconductor Integrated Technology, Institute of Semiconductors, Chinese Academy of Sciences, Beijing, 100083, China

[b] Center of Materials Science and Optoelectronics Engineering & School of Integrated Circuits, University of Chinese Academy of Sciences, Beijing, 100049, China

[c] Beijing Engineering Research Center of Semiconductor Micro-Nano Integrated Technology, Beijing, 100083, China

ARTICLE INFO

Keywords:
$InAs/GaAs_{0.8}Sb_{0.2}$ QDSCs
Irradiation resistance
Displacement per atom

ABSTRACT

Particles in space cause irradiation damage to the solar cells (SCs), resulting in the degradation of their performance. Quantum dot solar cells (QDSCs) have higher theoretical efficiency and better irradiation resistance than the conventional GaAs SCs, which makes them highly promising for application in space. In this paper, we study the proton irradiation effect on $InAs/GaAs_{0.8}Sb_{0.2}$ QDSCs by SRIM program. The simulation result shows that the $InAs/GaAs_{0.8}Sb_{0.2}$ QDSCs have fewer vacancies than GaAs SCs when irradiated with low-energy proton, which indicates that the $InAs/GaAs_{0.8}Sb_{0.2}$ QDSCs have better anti-irradiation characteristics. The study about displacements per atom and proton concentration in two SCs shows that protons with low energy and high irradiation fluences will cause more serious damage in $InAs/GaAs_{0.8}Sb_{0.2}$ QDSCs. In addition, the proton incident angle affects the vacancy distribution, while the number of QD layers has little effect on it.

1. Introduction

There are a large number of charged particles such as protons and electrons in space, which cause irradiation damage to optoelectronic devices in space, leading to a degradation of their performance [1,2]. However, the three-dimensional confinement properties of quantum dots (QDs) make them have good irradiation resistance, which has been confirmed in QD detectors and QD lasers [3–6]. A. Aierken et al. found that the photoluminescence (PL) intensity of GaAs degraded the most, quantum wells followed and InGaAs/GaAs QDs decreased the least under the same irradiation condition [7]. Also, there are some relevant studies in QDSCs. Cory D. Cress et al. also found that the InAs/GaAs QDSC maintains a much greater normalized V_{oc} compared to the SC without QDs, which suggests that the QDs improve the irradiation resistance of the device [8,9]. The study of Takeshi Ohshima et al. also supports that QDSCs have better anti-irradiation performance, and they found the J_{sc} recovered after annealing at room temperature [10–12]. In

* Corresponding author. Engineering Research Center for Semiconductor Integrated Technology, Institute of Semiconductors, Chinese Academy of Sciences, Beijing, 100083, China.

** Corresponding author. Engineering Research Center for Semiconductor Integrated Technology, Institute of Semiconductors, Chinese Academy of Sciences, Beijing, 100083, China.

E-mail addresses: liuwen519@semi.ac.cn (W. Liu), xdwang@semi.ac.cn (X. Wang).

https://doi.org/10.1016/j.heliyon.2024.e33910
Received 22 February 2024; Received in revised form 14 June 2024; Accepted 28 June 2024
Available online 28 June 2024

addition, the QDSC can absorb the low-energy photons through the intermediate band, and it has a theoretical efficiency as high as 63.2 % [13,14]. The good irradiation resistance and ultra-high theoretical efficiency of QDSCs make them potentially applicable in space [15,16].

The QDSCs can be categorized into type I and type II QDSCs. In type II QDSCs, the electrons and holes are spatially separated, suppressing carrier recombination in the QDs and increasing the carrier lifetime [17,18]. Specifically, for the InAs/GaAsSb QDSC, it begins to exhibit a type II band structure when the content of Sb exceeds 14 % [19,20]. A conversion efficiency of 17.31 % is achieved when the Sb content reaches 18 % [21]. The carrier lifetime can be further prolonged by adding a GaAs interlayer between the InAs QDs and GaAsSb layers [22]. The spatial separation of carriers in InAs/GaAsSb type II QDSCs may further bolster their irradiation resistance.

In this paper, the irradiation effect on InAs/$GaAs_{0.8}Sb_{0.2}$ QDSCs was investigated and the mechanisms that contribute to the good irradiation resistance were studied. Initially, the electron and nuclear stopping power of InAs and $GaAs_{0.8}Sb_{0.2}$ materials, as well as the influence of Sb content, was examined. Subsequently, the energy loss, vacancy distribution, proton distribution, and displacement per atom in InAs/$GaAs_{0.8}Sb_{0.2}$ QDSCs and GaAs SCs were compared, which proved that the InAs/$GaAs_{0.8}Sb_{0.2}$ QDSCs have excellent irradiation resistance. Finally, the impact of varying proton incident angles and the number of InAs/$GaAs_{0.8}Sb_{0.2}$ layers on their irradiation performance was studied.

2. Introduction to the SRIM program

In contrast to simulation software used in the irradiation study of SCs, such as PC1D, wxAMPS, and COMSOL, SRIM is a program designed to simulate the interaction between ion beam and solids [23–26]. By simulating the movement of incident particles, SRIM stores information about particle position, energy loss and various parameters of secondary particles throughout the entire tracking process. Finally, it calculates the expected value of various required physical quantities and corresponding statistical errors [26–28]. The SRIM consists of two main programs: the Tables of Stopping and Ranges of Ions in Matter (SR) and the Transport of Ions in Matter (TRIM). SR can quickly generate Tables of Stopping and Range of Ions in matter across a wide range of ion energies. TRIM, on the other hand, performs detailed calculations of the energy transferred during every collision with a target atom.

In this paper, the evaluation of irradiation damage in InAs/$GaAs_{0.8}Sb_{0.2}$ QDSCs and reference GaAs SCs mainly relies on two parameters: displacements per atom (DPA) and proton concentration (C). DPA denotes the displacements per atom under a given irradiation condition. The concentration reflects the distribution of irradiated particles within the material. Their equations are as follows [29]:

$$C = \frac{F(ion/cm^2) \times (atoms/cm^3)/(atoms/cm^2)}{N_0(atoms/cm^3)} \times 100 \tag{1}$$

$$DPA = R\left(\frac{vacancies}{ion \times A}\right) \times \frac{F(ion/cm^2)}{N_0(atoms/cm^3)} \times 10^8 \tag{2}$$

where F is the irradiation fluence, R is the average number of vacancies produced per unit distance by each incident particle, which can be obtained from the output file vacancy.txt of the TRIM program. (atoms/cm^3)/(atoms/cm^2) can be obtained from the output file range.txt, and N_0 is the atomic number density of the target materials. The number of protons used in this study is 10000.

Fig. 1 shows the structure of the InAs/$GaAs_{0.8}Sb_{0.2}$ QDSCs and GaAs SCs used in this research. The structure refers to the SCs structure described in reference [30]. The InAs QD layer has a thickness of 1.8 nm and is capped by a 10 nm $GaAs_{0.8}Sb_{0.2}$ layer. The thicknesses of the contact layer, emitter layer, base layer, and buffer layer are 50 nm, 150 nm, 500 nm, and 300 nm, respectively. In this study, protons are injected into the cells from the contact layer.

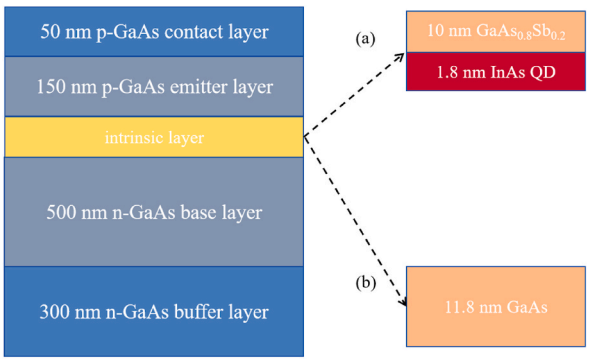

Fig. 1. The schematic diagram of the InAs/$GaAs_{0.8}Sb_{0.2}$ QDSCs **(a)** and the GaAs SCs **(b)**.

3. The irradiation damage in InAs/GaAsSb QDSCs

3.1. The energy loss and vacancy distribution

Fig. 2 depicts the variation of electron stopping power and nuclear stopping power with proton energy in GaAsSb and InAs layers, and the proton energy ranges from 10 keV to 10 MeV. For InAs/GaAsSb QDSCs, the Sb content is crucial in the formation of intermediate band solar cells. We initially simulated the energy losses of InAs layers and GaAsSb layers with different Sb contents. As the proton irradiation energy increases, the energy loss of these materials displays the same tendency. Their electronic stopping power initially increases and then decreases, while the nuclear stopping power continuously decreases. Additionally, as the Sb content increases, both the electronic stopping power and nuclear stopping power of GaAsSb materials decrease.

Fig. 3 shows the variation of phonon energy loss and ionization energy loss with proton energy in InAs/$GaAs_{0.8}Sb_{0.2}$ QDSCs and GaAs SCs, and the proton energy ranges from 10 keV to 3 MeV. The energy loss of the two SCs are dominated by ionization energy loss and show the same tendency with the variation of proton energy. As the proton energy increases, the proportion of ionization energy loss progressively increases, while the proportion of phonon energy loss diminishes. And the energy loss in the two SCs reaches stability under high-energy proton irradiation. This is because that if the proton energy is high enough, the majority of the protons will penetrate the entire SCs, reducing the collision between protons and lattice atoms, and consequently reducing the energy transfer to phonons. It is worth noting that the primary distinction between the two SCs lies in their response to low-energy proton irradiation. The proportion of phonon energy loss in InAs/$GaAs_{0.8}Sb_{0.2}$ QDSCs is smaller than that in GaAs SCs when they are irradiated with low-energy protons. Since the phonon energy loss is correlated with the generation of vacancies, the results above indicates that InAs/$GaAs_{0.8}Sb_{0.2}$ QDSCs have better irradiation resistance compared to GaAs SCs under low-energy proton irradiation.

Fig. 4 shows the variation of vacancy distribution with proton energy in InAs/$GaAs_{0.8}Sb_{0.2}$ QDSCs and GaAs SCs, and the proton energy is the same as in Fig. 3. The two SCs exhibit a similar trend as proton energy increases. Initially, the increase of proton energy leads to a rise in the energy transfer to phonon, resulting in the creation of vacancies. However, once the proton energy reaches a threshold and the proton can penetrate the entire SCs, a notable decrease in the number of vacancies will be observed. Additionally, both SCs exhibit comparable irradiation resistance under high-energy proton irradiation, which suggests that the contribution of quantum dots to the anti-irradiation performance will be not significant if the proton energy is too high. Specifically, the number of vacancies in InAs/$GaAs_{0.8}Sb_{0.2}$ QDSCs and GaAs SCs are 9.1 and 9.9 at 50 keV, respectively, and 11.4 and 12.6 at 150 keV. When the proton irradiation energy reaches 1 MeV, the vacancy drops to 0.8 for both SCs. Therefore, InAs/$GaAs_{0.8}Sb_{0.2}$ QDSCs exhibit less damage than GaAs SCs under low-energy irradiation, indicating that they have superior irradiation resistance. Besides, the results

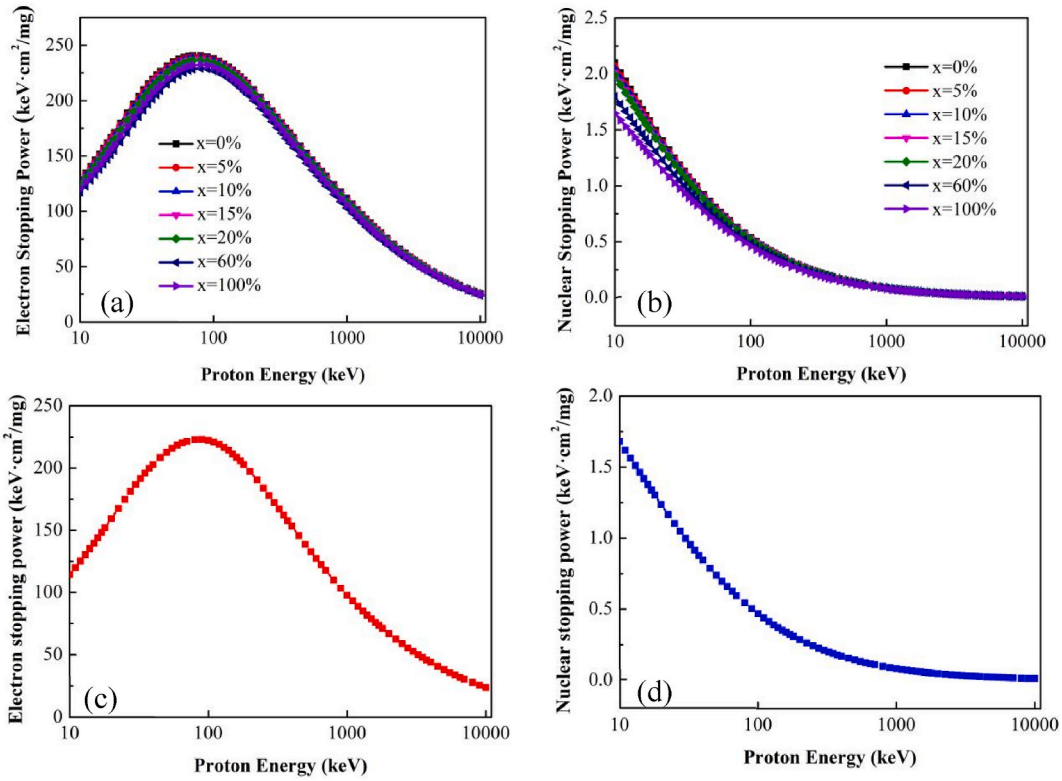

Fig. 2. The variation of electron stopping power **(a)** and nuclear stopping power **(b)** with proton energy in $GaAs_{1-x}Sb_x$ layers; the variation of electron stopping power **(c)** and nuclear power **(d)** with proton energy in InAs layers.

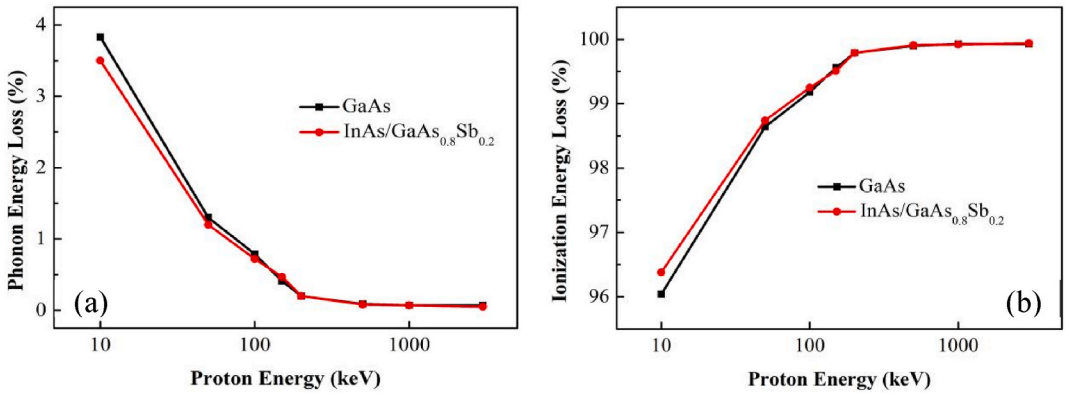

Fig. 3. The variation of phonon energy loss **(a)** and ionization energy loss **(b)** with proton energy.

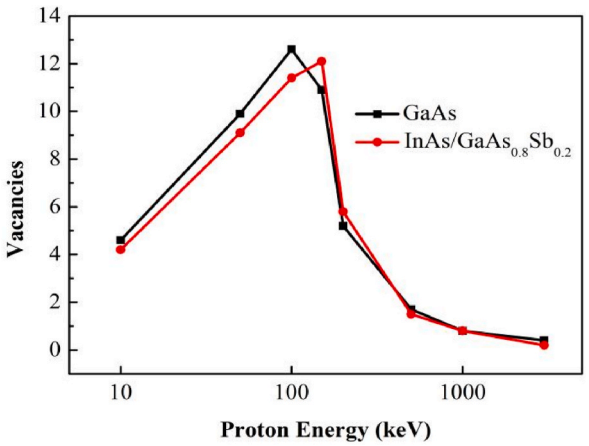

Fig. 4. Variation of vacancy distribution with proton energy.

suggest that low-energy proton irradiation causes more severe damage in both SCs, which is consistent with the conclusion in reference [31].

Notably, there is a peak shift in Fig. 4 and the InAs/$GaAs_{0.8}Sb_{0.2}$ QDSCs have more vacancies than GaAs SCs when the proton energy is 200 keV. The addition of the quantum dots decreases the number of vacancies behind the QD layer, while it hinders the movement of the proton, which can also be observed in Fig. 5. The energy required for protons to penetrate the GaAs SCs is approximately 150 keV, while the protons with the same energy are unable to penetrate the InAs/$GaAs_{0.8}Sb_{0.2}$ QDSCs. And once the proton can permeate the entire SCs, the number of vacancies will be significantly reduced.

Fig. 5 shows the variation of vacancy distribution in InAs/$GaAs_{0.8}Sb_{0.2}$ QDSCs and GaAs SCs, and the proton energy is 50 keV in Fig. 5 (a) and Fig. 5 (d), 150 keV in Fig. 5 (b) and Fig. 5 (e), 1 MeV in Fig. 5 (c) and Fig. 5 (f). As observed from Fig. 5, the ranges of proton within the two SCs increase with the rise of proton irradiation energy, resulting in a deeper position of the vacancies. Besides, there is a notable reduction in the number of vacancies behind the QD layer. The integration of vacancy reveals that the total number of vacancies in the InAs/$GaAs_{0.8}Sb_{0.2}$ QDSCs decreases by approximately 8.3 % compared to the GaAs SCs. However, it is noteworthy that there are more vacancies in InAs/$GaAs_{0.8}Sb_{0.2}$ QDSC at the surface and the total number of vacancies in front of the InAs and $GaAs_{0.8}Sb_{0.2}$ layers increases by about 8.9 %. This is because that the movement of protons is impeded by the QD and $GaAs_{0.8}Sb_{0.2}$ layers. Furthermore, Fig. 5 (b) and Fig. 5 (e) verify that protons with 150 keV energy can penetrate the GaAs SCs while they are unable to penetrate the InAs/$GaAs_{0.8}Sb_{0.2}$ QDSCs. When the proton energy reaches 1 MeV, most protons penetrate the two SCs, resulting in fewer vacancies and a more uniform distribution.

3.2. The DPA and proton distribution

Fig. 6 and Fig. 7 show the variation of the DPA with proton fluence in InAs/$GaAs_{0.8}Sb_{0.2}$ QDSCs and GaAs SCs under 50 keV and 150 keV proton irradiation. As the irradiation fluence rises, the DPA of both SCs increases, suggesting that high irradiation fluence will cause more severe damage to the SCs. The DPA initially increases and then decreases in GaAs SCs under 50 keV proton irradiation. When the proton energy increases to 150 keV, the maximum DPA shifts to a deeper position. Different from GaAs SCs, there is a

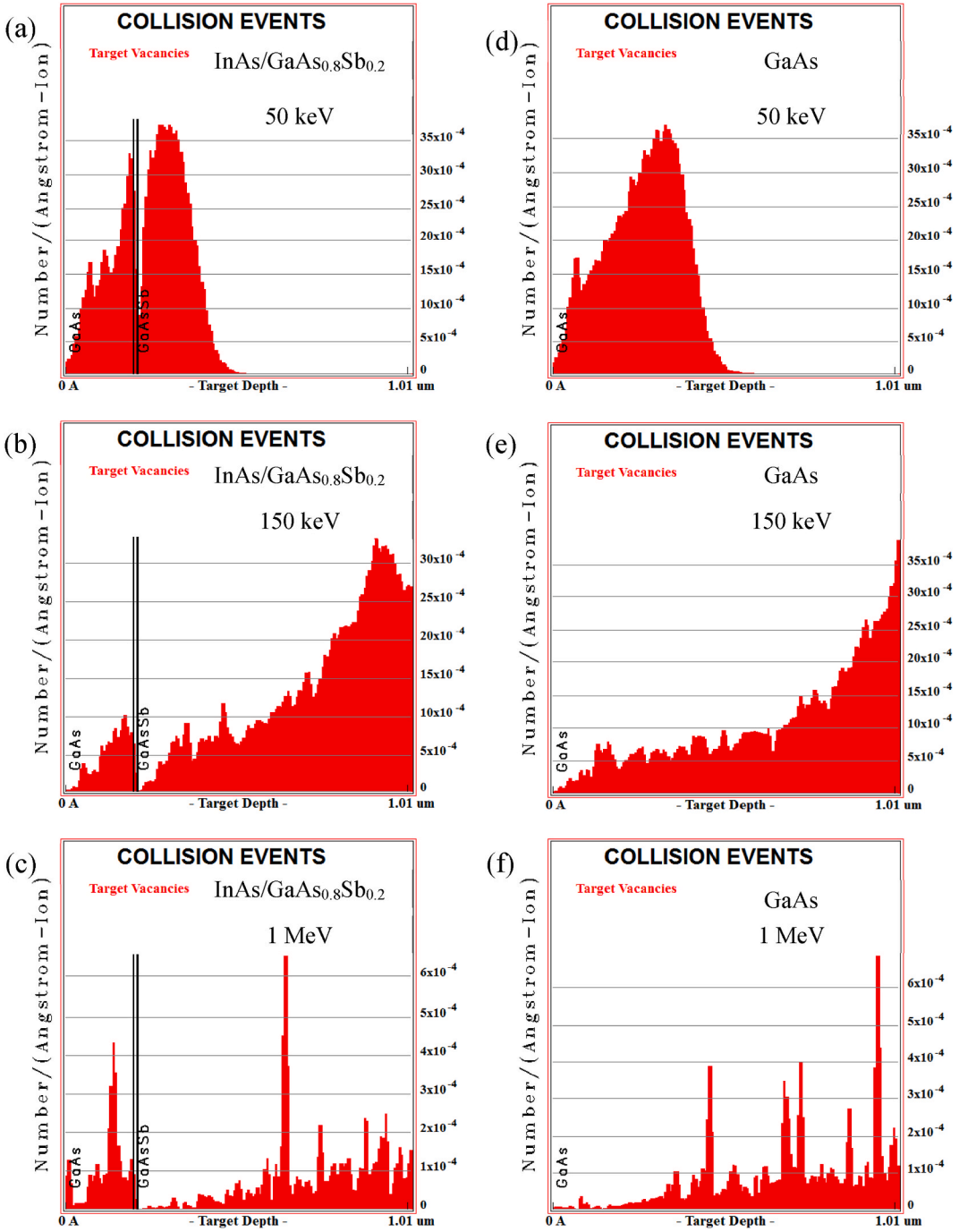

Fig. 5. The variation of vacancy distribution in SCs. **(a)**, **(b)** and **(c)** are the InAs/$GaAs_{0.8}Sb_{0.2}$ QDSCs; **(d)**, **(e)** and **(f)** are the GaAs SCs. The two black lines in the left graphs are InAs and $GaAs_{0.8}Sb_{0.2}$ layers.

noticeable decrease in the DPA within the range of 0.19224 μm–0.2226 μm (50 keV) and 0.18213 μm–0.2216 μm (150 keV) in InAs/$GaAs_{0.8}Sb_{0.2}$ QDSCs, which corresponds to the InAs QDs and $GaAs_{0.8}Sb_{0.2}$ layers. Furthermore, the maximum DPA of the InAs/$GaAs_{0.8}Sb_{0.2}$ QDSCs decreases with the increase of proton energy, dropping from 0.77 to 0.69 at 1×10^{17} H^+/cm^{-2}, while the maximum DPA in GaAs SCs has hardly changed, which proves that InAs/$GaAs_{0.8}Sb_{0.2}$ QDSCs have better irradiation resistance than GaAs SCs.

Fig. 8 and Fig. 9 show the variation of the proton concentration with irradiation fluence under 50 keV and 150 keV proton irradiation in InAs/$GaAs_{0.8}Sb_{0.2}$ QDSCs. The proton distribution in the two SCs is very similar, so only the change in InAs/$GaAs_{0.8}Sb_{0.2}$

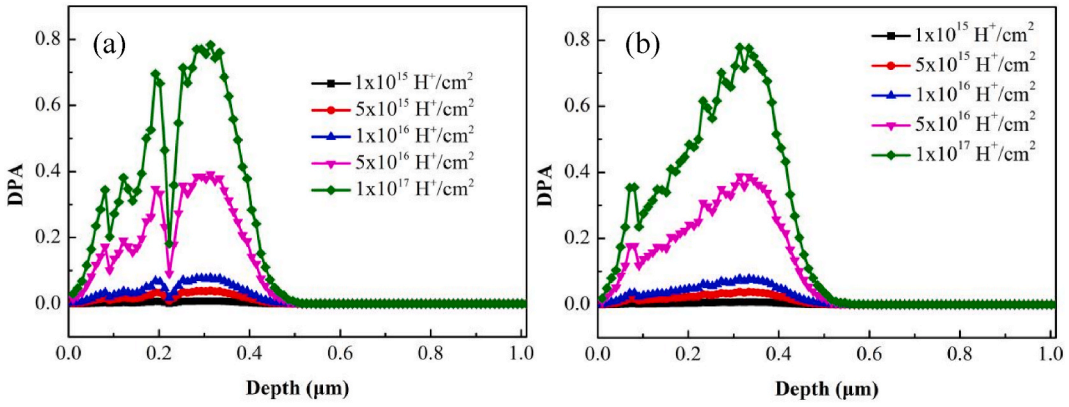

Fig. 6. The variation of the DPA with proton fluence under 50 keV proton irradiation in InAs/$GaAs_{0.8}Sb_{0.2}$ QDSCs **(a)** and in GaAs SCs **(b)**.

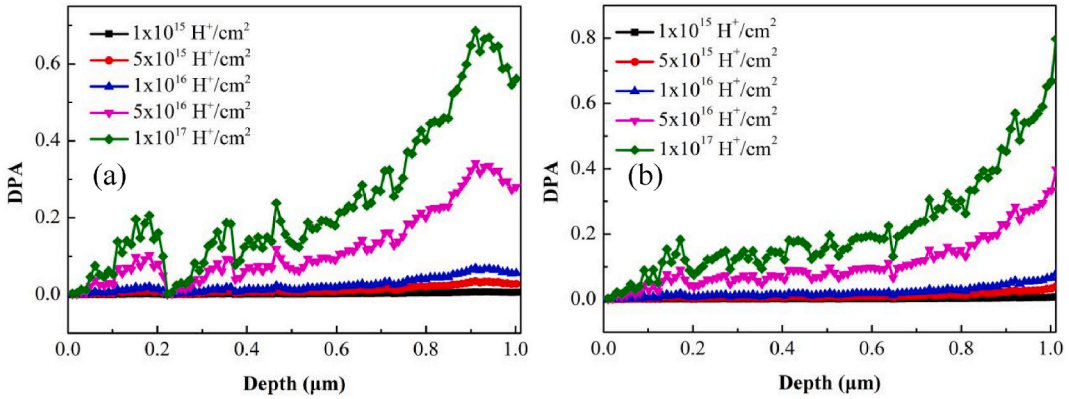

Fig. 7. The variation of the DPA with proton fluence under 150 keV proton irradiation in InAs/$GaAs_{0.8}Sb_{0.2}$ QDSCs **(a)** and in GaAs SCs **(b)**.

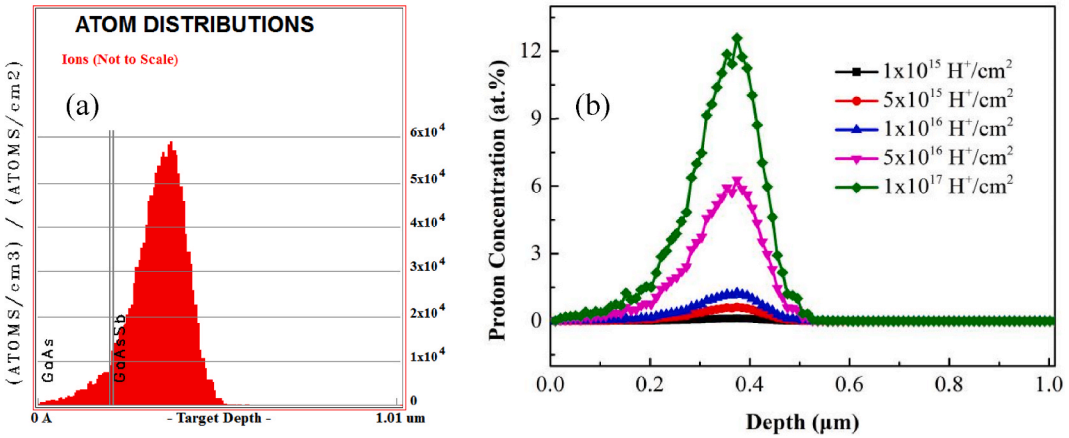

Fig. 8. The distribution of proton **(a)** and the variation of proton concentration with proton fluence **(b)** in InAs/$GaAs_{0.8}Sb_{0.2}$ QDSCs under 50 keV proton irradiation.

QDSCs is calculated here. When the QDSCs are irradiated with 50 keV protons, the proton concentration increases with the rise of irradiation fluence and reaches a maximum value of 0.13 at an irradiation fluence of 1×10^{15} H^+/cm^2, 6.29 at 5×10^{16} H^+/cm^2, and 12.58 at 1×10^{17} H^+/cm^2. The position of the maximum concentration remains unchanged and the depth is about 0.37 μm. The variation of concentration with proton fluence under 150 keV proton irradiation is similar to that under 50 keV proton irradiation, and there are two main differences. The position of the maximum concentration deepens and the depth is about 1 μm under 150 keV proton

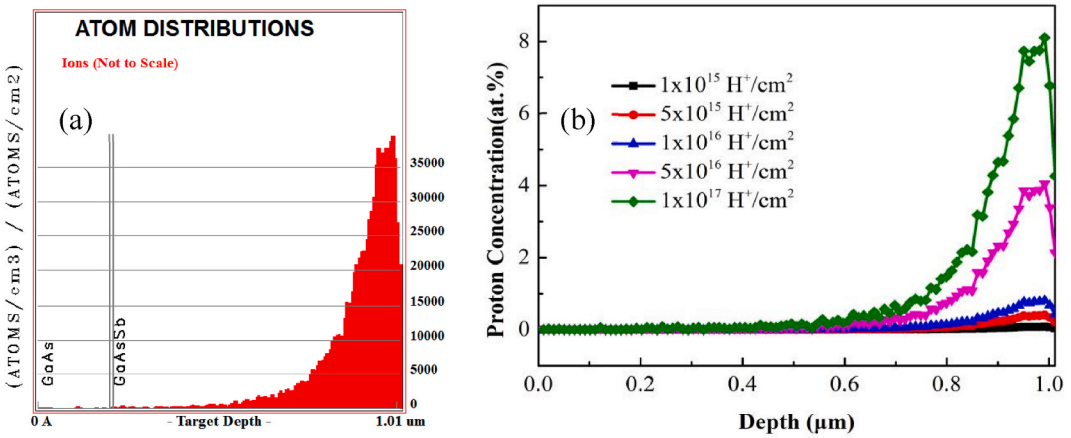

Fig. 9. The distribution of proton **(a)** and the variation of proton concentration with proton fluence **(b)** in InAs/$GaAs_{0.8}Sb_{0.2}$ QDSCs under 150 keV proton irradiation.

irradiation. Additionally, as the proton energy increases, the maximum concentration decreases, for example, it drops by 35.6 % at an irradiation fluence of 1×10^{17} H^+/cm^2. The findings above indicate that proton with low energy and high irradiation fluence causes more severe damage in QDSCs, and the simulation results are in agreement with reference [31].

3.3. *The influence of proton incidence angles and the number of QD layers*

Fig. 10 shows the variation of vacancy distribution with proton incidence angle under 100 keV proton irradiation in InAs/$GaAs_{0.8}Sb_{0.2}$ QDSCs. With the increase of the proton incident angle, the peak of the vacancy distribution shifts toward the surface, which is caused by the shortening of the proton projection range. The peak position is 0.65 μm at 0°, 0.57 μm at 30°, and 0.28 μm at 60°. When the proton incidence angle reaches 89.9°, the vacancies are distributed only on the surface. The integration results indicate that the total number of vacancies remains unchanged when the incident angle is within the range of 0°–60°. However, the number of vacancies decreases when the angle increases to 89.9°. The reason may be that when the proton incident angle is too large, some protons don't get into the SCs.

Fig. 11 illustrates the variation of vacancy distribution with the number of QD layers under 100 keV proton irradiation in InAs/$GaAs_{0.8}Sb_{0.2}$ QDSCs. It can be observed from Fig. 11 (a) that the average range of protons is less than the thickness of the QDSCs, and the vacancy distribution hardly changes with increasing the number of QD layers. Fig. 11 (b) shows the change of vacancy distribution in the QD region, and it shows that the minimum value of the vacancies shifts to a deeper position when the number of QD layers increases, about 0.01–0.02 μm for every two additional QD layers, which is quite small compared to the thickness of the SCs. Additionally, there is an increase in vacancies in the 10-stacked InAs/$GaAs_{0.8}Sb_{0.2}$ QDs layers compared to that in the single layer. The QD layers impede the movement of protons and the 10-stack QD layers are thicker than the single layer, both of which result in more vacancies in 10-stacked InAs/$GaAs_{0.8}Sb_{0.2}$ QDSCs. Some researches show that the increase of QD layers enhances irradiation resistance of QDSCs [9]. The reason why the simulation results here differ from the reported experiment results may be that the enhancement is

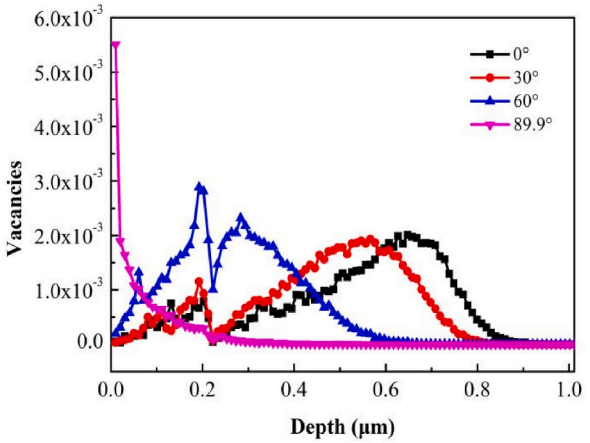

Fig. 10. The variation of vacancy distribution with proton incidence angle under 100 keV proton irradiation.

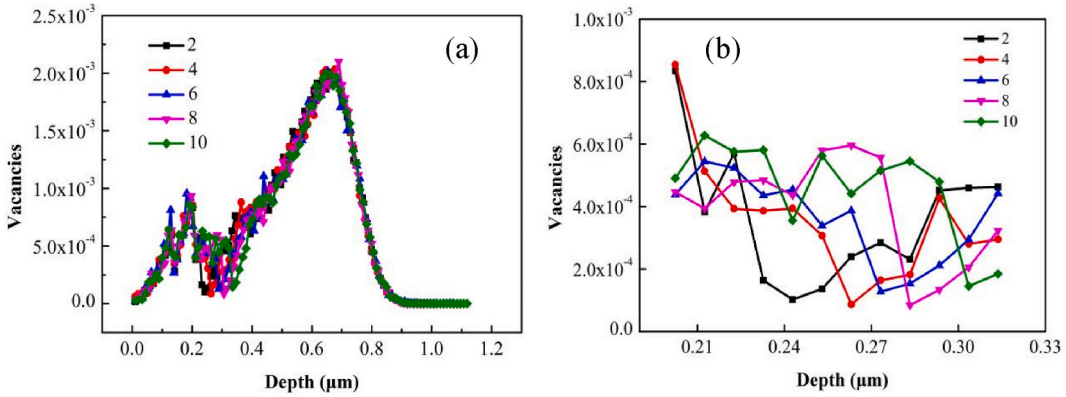

Fig. 11. The variation of vacancy distribution with the number of QD layers within the range of 0–1 μm **(a)** and 0.20–0.31 μm **(b)**.

related to the three-dimensional confinement characteristics of QDs, while we only consider the material properties in this paper. More research is needed to understand the irradiation resistance of QDSCs.

4. Conclusion

The proton irradiation effect on InAs/$GaAs_{0.8}Sb_{0.2}$ QDSCs is studied by SRIM simulation. The results show that the energy loss of InAs/$GaAs_{0.8}Sb_{0.2}$ QDSCs is mainly dominated by the ionization energy loss. There is less phonon energy loss and fewer vacancies in InAs/$GaAs_{0.8}Sb_{0.2}$ QDSCs than that in GaAs SCs under low-energy proton irradiation, which proves that InAs/$GaAs_{0.8}Sb_{0.2}$ QDSCs have better irradiation resistance. Besides, the DPA and proton concentration increase with the rise of proton irradiation fluence, and the DPA of the InAs/$GaAs_{0.8}Sb_{0.2}$ QDSC drops from 0.77 to 0.69 when proton energy increases from 50 keV to 150 keV, which indicates that proton with low energy and high irradiation fluence causes more serious irradiation damage in SCs. The peak of vacancy moves from 0.65 μm to the surface and the total number of vacancies is reduced when the proton incident angle increases from 0° to 89.9°. From the perspective of material properties, the number of QD layers hardly has an impact on the vacancy distribution in InAs/$GaAs_{0.8}Sb_{0.2}$ QDSCs. All in all, the InAs/$GaAs_{0.8}Sb_{0.2}$ QDSCs exhibit excellent irradiation resistance and have the potential for application in space.

Data availability statement

Data will be made available on request.

CRediT authorship contribution statement

Guiqiang Yang: Writing – original draft. **Yidi Bao:** Data curation. **Xiaoling Chen:** Investigation. **Chunxue Ji:** Data curation. **Bo Wei:** Data curation. **Wen Liu:** Writing – review & editing. **Xiaodong Wang:** Writing – review & editing.

Declaration of competing interest

The authors declare that they have no known competing financial interests or personal relationships that could have appeared to influence the work reported in this paper.

Acknowledgments

This research was supported by the National Key R&D Program of China (No. 2019YFB1503602).

References

[1] J. He, Y. Shen, B. Li, X. Xiang, S. Li, X. Fang, H. Xiao, X. Zu, L. Qiao, A comparative study of the structural and optical properties of Si-doped GaAs under different ion irradiation, Opt. Mater. 111 (2021) 110611, https://doi.org/10.1016/j.optmat.2020.110611.
[2] C. Gao, R. Cao, L. Li, B. Mei, H. Zhang, H. Lv, Y. Xue, X. Zeng, Proton irradiation effects on GaInP/GaAs/Ge triple junction cells, Opt. Mater. 142 (2023) 114006, https://doi.org/10.1016/j.optmat.2023.114006.
[3] S. Oktyabrsky, V. Tokranov, M. Yakimov, A. Sergeev, V. Mitin, in: E.W. Taylor, D.A. Cardimona, R.G. Pirich, N.S. Prasad, J. Pérez-Moreno, N.J. Dawson (Eds.), Nanoengineered Quantum Dot Medium for Space Optoelectronic Devices, 2012 851907, https://doi.org/10.1117/12.967124. San Diego, California, USA.
[4] C. Ribbat, R. Sellin, M. Grundmann, D. Bimberg, N.A. Sobolev, M.C. Carmo, Enhanced radiation hardness of quantum dot lasers to high energy proton irradiation, Electron. Lett. 37 (2001) 174, https://doi.org/10.1049/el:20010118.
[5] R. Leon, S. Marcinkecius, J. Siegert, B. Cechavicius, B. Magness, W. Taylor, C. Lobo, Effects of proton irradiation on luminescence emission and carrier dynamics of self-assembled III-V quantum dots, IEEE Trans. Nucl. Sci. 49 (2002) 2844–2851, https://doi.org/10.1109/TNS.2002.806018.

[6] Chi Che, Liu Qing-Feng, Ma Jing, Zhou Yan-Ping, National Key Laboratory of Tunable Laser Technology, Harbin Institute of Technology, Harbin 150001, China, Displacement damage effects on the characteristics of quantum dot lasers, Acta Phys. Sin. 62 (2013) 094219, https://doi.org/10.7498/aps.62.094219.
[7] A. Aierken, Q. Guo, T. Huhtio, M. Sopanen, ChF. He, Y.D. Li, L. Wen, D.Y. Ren, Optical properties of electron beam and γ-ray irradiated InGaAs/GaAs quantum well and quantum dot structures, Radiat. Phys. Chem. 83 (2013) 42–47, https://doi.org/10.1016/j.radphyschem.2012.09.022.
[8] C.D. Cress, C.G. Bailey, S.M. Hubbard, D.M. Wilt, S.G. Bailey, R.P. Raffaelle, Radiation effects on strain compensated quantum dot solar cells, in: 2008 33rd IEEE Photovolatic Spec. Conf., IEEE, San Diego, CA, USA, 2008, pp. 1–6, https://doi.org/10.1109/PVSC.2008.4922695.
[9] C.D. Cress, S.M. Hubbard, B.J. Landi, R.P. Raffaelle, D.M. Wilt, Quantum dot solar cell tolerance to alpha-particle irradiation, Appl. Phys. Lett. 91 (2007) 183108, https://doi.org/10.1063/1.2803854.
[10] T. Ohshima, S. Sato, T. Nakamura, M. Imaizumi, T. Sugaya, K. Matsubara, S. Niki, A. Takeda, Y. Okano, Electrical performance degradation of GaAs solar cells with InGaAs quantum dot layers due to proton irradiation, in: 2013 IEEE 39th Photovolt. Spec. Conf. PVSC, IEEE, Tampa, FL, USA, 2013, pp. 2779–2783, https://doi.org/10.1109/PVSC.2013.6745049.
[11] T. Ohshima, S. Sato, M. Imaizumi, T. Nakamura, T. Sugaya, K. Matsubara, S. Niki, Change in the electrical performance of GaAs solar cells with InGaAs quantum dot layers by electron irradiation, Sol. Energy Mater. Sol. Cells 108 (2013) 263–268, https://doi.org/10.1016/j.solmat.2012.09.027.
[12] T. Ohshima, S. Sato, C. Morioka, M. Imaizumi, T. Sugaya, S. Niki, Change in the electrical performance of InGaAs quantum dot solar cells due to irradiation, in: 2010 35th IEEE Photovolt, Spec. Conf., IEEE, Honolulu, HI, USA, 2010, pp. 2594–2598, https://doi.org/10.1109/PVSC.2010.5614152.
[13] A. Luque, A. Marti, Increasing the efficiency of ideal solar cells by photon induced transitions at intermediate levels, Phys. Rev. Lett. 78 (1997) 5014–5017, https://doi.org/10.1103/PhysRevLett.78.5014.
[14] I. Ramiro, A. Marti, E. Antolin, A. Luque, Review of experimental results related to the operation of intermediate band solar cells, Ieee J. Photovolt. 4 (2014) 736–748, https://doi.org/10.1109/JPHOTOV.2014.2299402.
[15] N. Žurauskienė, S. Ašmontas, A. Dargys, J. Kundrotas, G. Janssen, E. Goovaerts, S. Marcinkevičius, P.M. Koenraad, J.H. Wolter, R.P. Leon, Semiconductor nanostructures for infrared applications, Solid State Phenom. 99–100 (2004) 99–108, https://doi.org/10.4028/www.scientific.net/SSP.99-100.99.
[16] G.M. Dalpian, J.R. Chelikowsky, Self-purification in semiconductor nanocrystals, Phys. Rev. Lett. 96 (2006) 226802, https://doi.org/10.1103/PhysRevLett.96.226802.
[17] L. Cuadra, A. Marti, A. Luque, Type II broken band heterostructure quantum dot to obtain a material for the intermediate band solar cell, Phys. E-Low-Dimens. Syst. Nanostructures 14 (2002) 162–165, https://doi.org/10.1016/S1386-9477(02)00370-3.
[18] F. Xu, X.-G. Yang, S. Luo, Z.-R. Lv, T. Yang, Enhanced performance of quantum dot solar cells based on type II quantum dots, J. Appl. Phys. 116 (2014) 133102, https://doi.org/10.1063/1.4895476.
[19] A.D. Utrilla, J.M. Ulloa, Ž. Gačević, D.F. Reyes, I. Artacho, T. Ben, D. González, A. Hierro, A. Guzman, Impact of alloyed capping layers on the performance of InAs quantum dot solar cells, Sol. Energy Mater. Sol. Cells 144 (2016) 128–135, https://doi.org/10.1016/j.solmat.2015.08.009.
[20] A.D. Utrilla, D.F. Reyes, J.M. Llorens, I. Artacho, T. Ben, D. González, Ž. Gačević, A. Kurtz, A. Guzman, A. Hierro, J.M. Ulloa, Thin GaAsSb capping layers for improved performance of InAs/GaAs quantum dot solar cells, Sol. Energy Mater. Sol. Cells 159 (2017) 282–289, https://doi.org/10.1016/j.solmat.2016.09.006.
[21] S. Wang, S. Wang, X. Yang, Z. Lv, H. Chai, L. Meng, T. Yang, Improved performance of quantum dot solar cells by type-II InAs/GaAsSb structure with moderate Sb composition, Heliyon 9 (2023) e20005, https://doi.org/10.1016/j.heliyon.2023.e20005.
[22] D. Kim, S. Hatch, J. Wu, K.A. Sablon, P. Lam, P. Jurczak, M. Tang, W.P. Gillin, H. Liu, Type-II InAs/GaAsSb quantum dot solar cells with GaAs interlayer, IEEE J. Photovolt. 8 (2018) 741–745, https://doi.org/10.1109/JPHOTOV.2018.2815152.
[23] S. Sato, H. Miyamoto, M. Imaizumi, K. Shimazaki, C. Morioka, K. Kawano, T. Ohshima, Degradation modeling of InGaP/GaAs/Ge triple-junction solar cells irradiated with various-energy protons, Sol. Energy Mater. Sol. Cells 93 (2009) 768–773, https://doi.org/10.1016/j.solmat.2008.09.044.
[24] Y. Liu, Y. Sun, A. Rockett, A new simulation software of solar cells—wxAMPS, Sol. Energy Mater. Sol. Cells 98 (2012) 124–128, https://doi.org/10.1016/j.solmat.2011.10.010.
[25] H. Mazouz, P.-O. Logerais, A. Belghachi, O. Riou, F. Delaleux, J.-F. Durastanti, Effect of electron irradiation fluence on the output parameters of GaAs solar cell, Int. J. Hydrog. Energy 40 (2015) 13857–13865, https://doi.org/10.1016/j.ijhydene.2015.05.127.
[26] S. Agarwal, Y. Lin, C. Li, R.E. Stoller, S.J. Zinkle, On the use of SRIM for calculating vacancy production: quick calculation and full-cascade options, Nucl. Instrum. Methods Phys. Res. Sect. B Beam Interact. Mater. At. 503 (2021) 11–29, https://doi.org/10.1016/j.nimb.2021.06.018.
[27] S.-L. Chen, Low-energy atomic displacement model of SRIM simulations, Nucl. Sci. Tech. 32 (2021) 119, https://doi.org/10.1007/s41365-021-00971-2.
[28] J.-P. Crocombette, C. Van Wambeke, Quick calculation of damage for ion irradiation: implementation in Iradina and comparisons to SRIM, EPJ Nucl. Sci. Technol. 5 (2019) 7, https://doi.org/10.1051/epjn/2019003.
[29] J. Zhou, R. Hao, X. Pan, Y. Ren, J. Li, J. Zhao, J. Kong, SRIM simulation of irradiation damage by protons in InAs/GaSb type-II superlattices, J. Kor. Phys. Soc. (2023), https://doi.org/10.1007/s40042-022-00689-3.
[30] W.-S. Liu, H.-M. Wu, F.-H. Tsao, T.-L. Hsu, J.-I. Chyi, Improving the characteristics of intermediate-band solar cell devices using a vertically aligned InAs/GaAsSb quantum dot structure, Sol. Energy Mater. Sol. Cells 105 (2012) 237–241, https://doi.org/10.1016/j.solmat.2012.06.023.
[31] D. Elfiky, M. Yamaguchi, T. Sasaki, T. Takamoto, C. Morioka, M. Imaizumi, T. Ohshima, S. Sato, M. Elnawawy, T. Eldesuky, A. Ghitas, Study the effects of proton irradiation on GaAs/Ge solar cells, in: 2010 35th IEEE Photovolt, Spec. Conf., IEEE, Honolulu, HI, USA, 2010, https://doi.org/10.1109/PVSC.2010.5614633, 002528–002532.